

1 **Title:** Heme uptake in *Lactobacillus sakei* evidenced by a new ECF-like transport system.

2

3 Emilie Verplaetse¹, Gwenaëlle André-Leroux², Philippe Duhutrel^{1,3}, Gwendoline Coeuret¹,

4 Stéphane Chaillou¹, Christina Nielsen-Leroux¹, Marie-Christine Champomier-Vergès^{1*}

5 1) Université Paris-Saclay, INRAE, AgroParisTech, Micalis Institute, 78350 Jouy-en-
6 Josas, France.

7 2) Université Paris-Saclay, INRAE, MaIAGE, 78350 Jouy-en-Josas, France.

8 3) Present address: bioMérieux, 5 rue des Aqueducs, 69290 Craponne, France.

9

10

11

12

13 Running title: heme transport in *Lactobacillus sakei*

14

15 *Corresponding author: marie-christine.champomier-verges@inra.fr

16

17 Key-words: iron, lactic acid bacteria, ABC-transporter

18

19 **Abstract**

20 *Lactobacillus sakei* is a non-pathogenic lactic acid bacterium and a natural inhabitant of meat
21 ecosystems. Although red meat is a heme-rich environment, *L. sakei* does not need iron or
22 heme for growth, while possessing a heme-dependent catalase. Iron incorporation into *L.*
23 *sakei* from myoglobin and hemoglobin was formerly shown by microscopy and the *L. sakei*
24 genome reveals a complete equipment for iron and heme transport. Here, we report the
25 characterization of a five-gene cluster (*lsa1836-1840*) encoding a putative metal iron ABC
26 transporter. Interestingly, this cluster, together with a heme dependent catalase gene, is also
27 conserved in other species from the meat ecosystem. Our bioinformatic analyses revealed
28 that the locus might refer to a complete machinery of an Energy Coupling Factor (ECF)
29 transport system. We quantified *in vitro* the intracellular heme in wild-type (WT) and in our
30 Δ *lsa1836-1840* deletion mutant using an intracellular heme sensor and ICP-Mass
31 spectrometry for quantifying incorporated ⁵⁷Fe heme. We showed that in the WT *L. sakei*,
32 heme accumulation occurs fast and massively in the presence of hemin, while the deletion
33 mutant was impaired in heme uptake; this ability was restored by *in trans* complementation.
34 Our results establish the main role of the *L. sakei* Lsa1836-1840 ECF-like system in heme
35 uptake. This research outcome shed new light on other possible functions of ECF-like
36 systems.

37

38

39 **Importance**

40 *Lactobacillus sakei* is a non-pathogenic bacterial species exhibiting high fitness in heme rich
41 environments such as meat products, although it does not need iron nor heme for growth.
42 Heme capture and utilization capacities are often associated with pathogenic species and are
43 considered as virulence-associated factors in the infected hosts. For these reasons, iron

44 acquisition systems have been deeply studied in such species, while for non-pathogenic
45 bacteria the information is scarce. Genomic data revealed that several putative iron
46 transporters are present in the genome of the lactic acid bacterium *L. sakei*. In this study, we
47 demonstrate that one of them, is an ECF-like ABC transporter with a functional role in heme
48 transport. Such evidence has not yet been brought for an ECF, therefore our study reveals a
49 new class of heme transport system.

50

51

52 **Introduction**

53

54 Iron is an essential element for almost all living organisms (1) and heme, an iron-containing
55 porphyrin, is both a cofactor of key cellular enzymes and an iron source for bacteria. Many
56 bacteria encode the complete heme biosynthesis pathway to be autonomous for heme
57 production and partly to guarantee their iron supply. However, some others lack heme
58 biosynthetic enzymes and rely on the environment to fulfill their heme requirements.

59 *Lactococcus lactis* and all known *Lactobacilli* are heme-auxotrophic bacteria (2). Also, it is
60 well established that lactic acid bacteria do not require iron to grow (3) and that their growth
61 is unaffected by iron deprivation. Nevertheless, numerous lactic acid bacteria, such as *L.*
62 *lactis*, *Lactobacillus plantarum*, or *Enterococcus faecalis*, require exogenous heme to activate
63 respiration growth in the presence of heme (2).

64 *Lactobacillus sakei* is a non-pathogenic lactic acid bacterium frequently found on fresh meat.
65 *L. sakei* becomes the predominant flora on vacuum packed meat stored at low temperature
66 (4). Interestingly, abundance of *L. sakei* has been shown to prevent growth of undesirable
67 pathogens such as *Listeria monocytogenes* (5, 6), *Escherichia coli* O157:H7 in both cooked
68 and smashed meat (5, 7, 8), and of spoilers such as *Brochothrix thermosfacta* (7, 8).

69 Therefore, this species is often used as a bioprotective culture in meat products. Nevertheless,
70 mechanisms of synergy and competition between species in such complex matrices are still
71 poorly understood (9). Meat, can be considered as a growth medium naturally rich in iron and
72 heme. Quantification of total iron content in raw meat reported a mean of 2.09 mg total
73 iron/100 g for four beef meat cuts in which 87% was heme iron (10). Although *L. sakei* had a
74 tropism for meat and is known to possess a heme-dependent catalase (11), it is considered to
75 be a bacterium that requires neither iron nor heme to grow.

76 First insights on iron/heme utilization by *L. sakei* came from its whole genome analysis (12)
77 with the identification of coding sequences of several iron transporters, regulators and iron-
78 containing enzymes. Later, microscopy analysis of *L. sakei* cells combined to spectroscopy
79 methods showed that *L. sakei* is able to incorporate iron atoms from complexed iron such as
80 myoglobin, hemoglobin, hematin, and transferrin (13). This suggested that *L. sakei* may
81 display heme or hemic-iron storage ability, although the analytical method used was not
82 quantitative and the precise amount of iron compound that *L. sakei* is able to store was not
83 determined. Hematin did not show any effect on growth of *L. sakei*, but hematin has been
84 shown to prolong bacteria viability in stationary phase (13). However, the mechanisms
85 underlining *L. sakei* survival in the presence of heme need to be unraveled.

86 Heme acquisition systems have mainly been studied in Gram-negative and Gram-positive
87 pathogens that acquire heme from host hemoproteins in a two steps process (for a review, see
88 (14–16)). First, cell surface or secreted proteins scavenge free heme molecules or complexed
89 heme. Then, transmembrane transporters, generally ATP-binding cassette (ABC) transporters,
90 carry the heme moiety into the intracellular space. Gram-positive bacteria rely mainly on
91 surface-exposed receptors that shuttle heme through the cell-wall and deliver it to an ABC
92 transporter for subsequent transfer into the cytoplasm. Within Gram-positive pathogens, one
93 of the most well characterized heme uptake system is the *Staphylococcus aureus* Iron Surface
94 Determinants (Isd) system. The staphylococcal machinery is inserted into a ten-gene locus
95 encoding cell-wall anchored proteins (IsdABCH), a membrane transport system (IsdDEF), a
96 sortase (SrtB) and two cytoplasmic heme-oxygenases (IsdG and IsdI) (17, 18). IsdB and IsdH
97 are responsible for binding host hemoproteins or heme. IsdA extracts heme from IsdB or IsdH
98 and transfers it to IsdC. Funneled heme is finally transferred into the cytoplasm through the
99 membrane by the IsdDEF ABC transporter where it is finally degraded to release free iron by
100 the heme oxygenases IsdG and IsdI. Several of these Isd proteins contain *Near* iron

101 Transporter (NEAT) domain, present only in Gram-positive bacteria, and specific to interact
102 with hemoproteins and heme. NEAT domain is a 150-acid residues domain that despite
103 sequence variability displays a conserved β -barrel and a hydrophobic pocket involved in
104 heme binding (19).

105 Thus far, heme acquisition systems in heme auxotrophic organisms have only been reported
106 for *Streptococci* (15, 20, 21). In *S. pyogenes*, the system involves the Shr and Shp NEAT-
107 domain proteins and the Hts ABC transporter (20, 22, 23). In *Lactococcus lactis*, heme
108 homeostasis, especially heme efflux systems, have been deeply characterized (24, 25).

109 Nevertheless, the acquisition of exogenous heme remains poorly characterized. Heme
110 transport across *L. sakei* membrane is still unknown. Additionally, bioinformatic analysis
111 shows that the genome of *L. sakei* does not contain any NEAT domain (12) which suggests
112 that heme transit could involve transport systems distinct from *Streptococci* and *S. aureus*
113 (14).

114 Regarding prokaryotic metal ion uptake transporters, comparative and functional genomic
115 analysis have identified Energy-Coupling Factor (ECF) transporters as a novel type of ABC
116 importers widespread in Gram-positive bacteria and first identified in lactic acid bacteria (26).

117 The studies identified genes encoding a ABC-ATPases plus three or four membrane proteins
118 within the same or adjacent to operons, which were implicated in vitamin production or
119 synthesis of metal-containing metalloenzymes (27). Their predicted role in cobalt or nickel
120 ions uptake and delivery within the cell was demonstrated in *Salmonella enterica* and
121 *Rhodococcus capsulatus*, respectively. Since then, ECF-coding genes have been evidenced in
122 *Mycoplasma*, *Ureaplasma* and *Streptococcus* strains. They were also shown to function as
123 importers not only for transition metal ions but also for vitamins as riboflavin and thiamine
124 (27). Recently, several ECF systems have been characterized, among them folate and
125 pantothenate ECF transport in *Lactobacillus brevis*, and cobalt ECF in *R. capsulatus* (28–31).

126 It was evidenced that ECF transporters constitute a novel family of conserved membrane
127 transporters in prokaryotes, while sharing a similar four domains organization as the ABC
128 transporters. Each ECF displays a pair of cytosolic nucleotide-binding ATPases (the A and A'
129 components also called EcfA and EcfA'), a membrane-embedded substrate-binding protein
130 (the S component or the EcfS), and a transmembrane energy-coupling component (The T
131 component or EcfT). The quadripartite organization has a 1:1:1:1 stoichiometry. Notably, the
132 S component renders ECF mechanistically distinct from ABC transport systems as it is
133 predicted to shuttle within the membrane, when carrying the bound substrate from the
134 extracellular side into the cytosol (see the recent review (26)). Accordingly, the S-component
135 solely confers substrate specificity to the uptake system (28). Till the 2000s, folate, riboflavin
136 and thiamine ECF importers have been reported for *L. lactis* (32–34). Similarly, folate,
137 hydroxyl pyrimidine and pantothenate ECFs have been reported and structurally characterized
138 for *L. brevis* (28, 30, 31), both Gram-positive rod shape species of lactic acid bacteria.
139 In this paper, we mainly targeted *L. sakei* locus *lsa1836-1840* encoding a putative ABC
140 transporter, and evaluated its role as a heme transport system, combining *in silico*
141 bioinformatics analysis with *in vitro* functional analysis. We showed that this system encodes
142 the complete machinery of an ECF-like importer, including the extracellular proteins that
143 initiate heme scavenging. Furthermore, we were able to dock heme at the binding site formed
144 by the interface of those two extracellular proteins that were homology modeled. In parallel,
145 we quantified the heme storage properties of *L. sakei*, and compared WT *L. sakei* with the
146 Δ *lsa1836-1840* *L. sakei* deletion mutant using an intracellular heme-reporter gene and mass-
147 spectrometry quantification of iron-labelled heme. We showed that *L. sakei* Δ *lsa1836-1840*
148 was strongly impaired in its ability to incorporate heme, while its complementation abolished
149 this phenotype. Additionally, when the *lsa1836-1840* genes were overexpressed, heme
150 incorporation was boosted. Thus, we were able to show *in vitro* that this five-gene locus plays

151 an important role in active heme import. To our knowledge, this is the first time that an ECF
152 is reported to being involved in heme incorporation.

153

154 **Results**

155

156 **1. Putative iron and heme transport systems in *Lactobacillus sakei***

157 Accurate analysis of the genome of *L. sakei* 23K (12), focused on heme/iron transport
158 systems and heme utilization enzymes, previously led to the identification of 5 putative iron
159 transport systems, five heme transport systems and one heme-degrading enzyme (Table 1).

160 First, two genes *lsa0246* and *lsa1699* encoding proton motive permeases, which belong to the
161 MntH family of manganese uptake, might be involved in iron or heme uptake. Notably, in *L.*
162 *lactis*, a *mntH* mutant was impaired in Fe²⁺ transport (35).

163 Second, an operon, composed of the genes *lsa1194-1195* coding for poorly defined
164 membrane proteins of the CCC1 family, is putatively involved in heme or iron transport. In
165 yeast, CCC1 is involved in the manganese and iron ions transport from the cytosol to the
166 vacuole for storage (36). Additionally, the gene *lsa1194*, has been shown to be upregulated in
167 a global transcriptomic analysis of genes differentially expressed in the presence of heme
168 (unpublished data).

169 Third, two ABC systems homologous to the HrtAB and Pef heme-detoxification systems
170 present in *L. lactis* and *Streptococcus agalactiae* (24, 37) were also identified in *L. sakei*
171 genome. These systems are encoded by the *lsa1366-1367* and *lsa0419-0420* genes,
172 respectively. The sequencing of the *lsa0419-0420* region has confirmed the presence of a
173 frameshift and indicated that these genes are not expressed in *L. sakei* 23K strain. The
174 *lsa1366-1367* gene products are homologous to the *L. lactis* *Llmg_0625-0624* encoded
175 proteins. The *L. lactis* genes code for the HrtB and HrtA proteins, respectively (24). An *in*

176 *silico* analysis of Lsa1367 and HrtB indicated that these proteins share 33% of sequence
177 identity and, accordingly, the same fold, as assessed by TOPPRED analysis (38). Particularly,
178 the cytoplasmic-exposed Y168 and Y231 amino-acid residues, shown as important for HrtB-
179 heme interaction in *L. lactis* (25), are also present in Lsa1367, which suggests that these genes
180 might be homologous to the *L. lactis* heme export system.

181 Last, two iron or heme uptake ABC-transporters were identified. Markedly, the operon
182 *lsa0399-0402* encodes a Fhu system, sharing homology with various orthologous genes and
183 operons encoding complexed iron transport systems, and possibly homologous to the *Listeria*
184 *monocytogenes* HupCGD system. Also, *L. monocytogenes* shows that HupCGD and Fhu are
185 involved in heme and ferrioxamine uptake, respectively (39).

186 Then, the ABC system encoded within *lsa1836-1840* genes was automatically annotated as
187 involved in cobalamin transport, whilst it shows some levels of similarities with heme import
188 systems described in Gram-positive bacteria (40–43). At first, we carried out a multiple
189 alignment of all putative substrate-binding lipoproteins encoded in the *L. sakei* 23K genome
190 and noticed that Lsa1839 protein was closely related to Lsa0399 from the Fhu system (data
191 not shown) suggesting a possible link to iron/heme transport. Furthermore, if heme
192 transportation would represent a specific fitness for growth in meat, we wondered whether
193 other meat-borne bacteria would contain a similar cluster in their genome. As shown in Figure
194 1, comparative genomic analysis revealed that the *lsa1836-1840* genes cluster is present in
195 several species known to harbor a tropism for meat. The most interesting observation is that
196 species harboring the *lsa1836-1840*-like cluster also have in their genome a *katA* gene,
197 encoding a heme dependent catalase, while the other species lacking the cluster, such
198 as *Leuconostoc* and *Lactococcus*, were shown to be deprived of catalase-encoding gene.
199 Although such co-occurrence could not constitute a proof of the role of the *lsa1836-1840*

200 cluster in heme transport, this analysis provided an additional argument consolidating this
201 hypothesis.

202

203 **2. The *lsa1836-1840* encodes an ECF like transport system putatively involved in heme** 204 **transport**

205 Due to the conservation of the operon *lsa1836-1840*, each of the five sequences was analyzed
206 comprehensively using bioinformatics. It includes multiple sequence alignment, as well as 3D
207 structure, proteins network and export peptide predictions. Lsa1836 shows a sequence
208 similarity of more than 30%, associated to a probability above 99% with an e-value of $8 \cdot e^{-15}$,
209 to share structural homology with the membrane-embedded substrate-binding protein
210 component S from an ECF transporter of the closely related *L. brevis*, as computed by
211 HHpred (44). Accordingly, its sequence is predicted to be an integral membrane component
212 with six transmembrane helices, and a very high rate of hydrophobic and apolar residues,
213 notably 11 tryptophan amino-acid residues among the 230 residues of the full-length protein
214 (Fig. 2A). HHpred analysis indicates that Lsa1837 shares more than 50 % sequence similarity
215 with the ATPase subunits A and A' of the same ECF in *L. brevis* (Fig. 2A). With 100% of
216 probability and a e-value of $1 \cdot e^{-35}$, Lsa1837 describes two repetitive domains, positioned at 9-
217 247 and 299-531, where each refers structurally to one ATPase very close in topology to the
218 solved ATPase subunits, A and A' of ECF from *L. brevis*, respectively. Appropriately, the N-
219 terminal and C-terminal ATPases, are predicted to contain an ATP-binding site. Lsa1837
220 could correspond to the fusion of ATPase subunits, A and A'. Protein Lsa1838 shows
221 sequence similarity of above 30%, with a probability of 100 % and e-value of $1 \cdot e^{-30}$, to share
222 structural homology with the membrane-embedded substrate-binding protein component T
223 from the ECF transporter of *L. brevis* (Fig. 2A). Interestingly, similar bioinformatic analysis
224 of sequence and structure prediction demonstrates that Lsa1839 and Lsa1840 share both

225 99.8% structural homology, and e-value of $1. e^{-24}$ and of $1. e^{-21}$, with the β and α domains of
226 human transcobalamin, respectively (Fig. 2A). Consistently, both proteins have an export
227 signal located at their N-terminal end. Taken together, these results predict with high
228 confidence that the transcriptional unit encodes the complete machinery of an ECF, including
229 the extracellular proteins that initiate the scavenging of iron-containing heme (Fig. 2A). Each
230 protein compartment is predicted through the presence/absence of its signal peptide as being
231 extracellular, embedded in the membrane or cytosolic. Correspondingly, every protein
232 sequence associates appropriate subcellular location with predicted function. In line with that,
233 the network computed by String for the set of proteins of the operon shows that they interact
234 together from a central connection related to Lsa1837, which corresponds to the ATP-motor
235 couple of ATPases (45). The transcriptional unit also encompasses Lsa1839 and Lsa1840,
236 highly homologous to β and α subunits of transcobalamin respectively, that are highly
237 hypothesized to initiate the scavenging of heme from the extracellular medium. To address
238 the capacity of those subunits of transcobalamin-like binding domain to bind a heme moiety,
239 we homology-modeled Lsa1839 and Lsa1840. We then assembled the biological unit
240 composed of the heterodimer formed by β and α subunits, using the related 3D templates of
241 corresponding subunit of haptocorrin and transcobalamin. Subsequently, an iron-containing
242 heme moiety was docked into the groove, located at the interface of the complex formed by
243 the two proteins. The redocking of cobalamin in haptocorrin and cyanocobalamin in
244 transcobalamin shows a binding energy of -17 and -12 kcal/mol, respectively (Fig. 2B). With
245 a binding energy of -9 kcal/mol, the heme bound to the crevice formed by Lsa1839 and
246 Lsa1840 displays an affinity in the same range than the endogenous ligands, and emphasizes
247 that the assembly composed of Lsa1839 and Lsa1840 could be compatible with the
248 recognition and binding of a heme (Fig. 2B). To resume, Lsa1836-1840 describes a complete
249 machinery that could be able to internalize a heme instead or additionally to a cobalamin

250 molecule. Importantly, this operon includes also the extracellular scavenging β - and α -like
251 subunits of transcobalamin, which advocates for that the S-component Lsa1836 is possibly
252 very specific for iron-containing heme. In line with that, despite a closely conserved fold, the
253 S-component does not display the strictly conserved residues known to bind cobalt-containing
254 cobalamin.

255 No heme synthesis enzymes are present in *L. sakei* genome, nevertheless a gene coding for a
256 putative heme-degrading enzyme of the Dyp-type peroxidase family, *lsa1831*, was identified
257 in the *L. sakei* genome. Its structure is predicted to be close to DypB from *Rhodococcus jostii*
258 (46). Interestingly, residues of DypB involved in the porphyrin-binding, namely Asp153,
259 His226 and Asn246, are strictly conserved in Lsa1831 (47). Markedly, the *lsa1831* gene is
260 located upstream of the *lsa1836-1840* operon putatively involved in the active heme transport
261 across the membrane.

262 Our bioinformatical analysis allows the functional reannotation of the *lsa1836-1840* genes
263 into the complete machinery of an Energy-Coupling Factor, possibly dedicated to the
264 transport of iron through the heme (Fig. 3A-B). Consistently, the Lsa1831 enzyme, which is
265 close to the *lsa1836-1840* loci, could participate downstream to release iron from the heme
266 once inside the cytoplasm.

267

268 **3. The Lsa1836-1840 is *in vitro* an effective actor of heme uptake in *L. sakei*.**

269 To confirm the above transporter as involved in heme trafficking across the membrane, a
270 *lsa1836-1840* deletion mutant was constructed by homologous recombination. The *L. sakei*
271 Δ *lsa1836-1840* mutant was analyzed for its capacity to internalize heme using an intracellular
272 heme sensor developed by Lechardeur and co-workers (24). This molecular tool consists in a
273 multicopy plasmid harboring a transcriptional fusion between the heme-inducible promoter of
274 *hrtR*, the *hrtR* coding sequence and the *lacZ* reporter gene, the pP_{hrt} *hrtR-lac* (Table 2). In *L.*

275 *lactis*, HrtR is a transcriptional regulator that represses the expression of a heme export
276 system, HrtA and HrtB, as well as its own expression in the absence of heme. Upon heme
277 binding, the repression is alleviated allowing the expression of the export proteins (24). As *L.*
278 *sakei* possesses the *lacLM* genes, it was necessary to construct the $\Delta lsa1836-1840$ mutant in
279 the *L. sakei* RV2002 strain, a *L. sakei* 23K $\Delta lacLM$ derivative, yielding the RV4057 strain
280 (Table 2). The pP_{hrt} *hrtR-lac* was then introduced in the RV2002 and RV4057 strains, yielding
281 the RV2002 *hrtR-lac* and the RV4057 *hrtR-lac* strains (Table 2). β -Galactosidase (β -Gal)
282 activity of the RV4057 *hrtR-lac* strain grown in a chemically defined medium (MCD) (48) in
283 the presence of 0.5, 1 and 5 μ M hemin was determined and compared to that of the RV2002
284 *hrtR-lac* used as control (Fig. 4A). We showed that hemin reached the intracellular
285 compartment as β -Gal expression was induced by hemin. Relative β -Gal activity of the
286 RV4057 *hrtR-lac* mutant strain showed a slight increase as compared to the WT at 0.5 μ M
287 heme but a statistically significant two-fold reduction was measured at 1 μ M heme and
288 further, a 40% reduced activity was shown at higher hemin concentration. This indicates that
289 the intracellular abundance of heme is significantly reduced in the RV4057 bacterial cells at 1
290 and 5 μ M heme, while it is similar to the WT at low heme concentrations. The method
291 described above did not allow to quantify the absolute amount of heme incorporated by
292 bacteria as only cytosolic heme may interact with HrtR. Therefore, we used hemin labeled
293 with the rare ⁵⁷iron isotope (⁵⁷Fe-Hemin) combined with Inductively Coupled Plasma Mass
294 Spectrometry (ICP-MS) to measure with accuracy the total heminic-iron content of cells.
295 Quantification of ⁵⁷Fe was used as a proxy to quantify heme. The absolute number of heme
296 molecules incorporated by the $\Delta lsa1836-1840$ mutant was also quantified using ⁵⁷Fe-hemin.
297 The $\Delta lsa1836-1840$ mutant was constructed in the WT *L. sakei* 23K genetic background to
298 obtain the RV4056 strain (Table 2). Bacteria were incubated in the MCD, in the absence or in
299 the presence of 1, 5 or 40 μ M of ⁵⁷Fe-hemin. ICP-MS quantification indicated that the ⁵⁷Fe

300 content of the two strains was similar at 1 μM ^{57}Fe -hemin. A 5-fold reduction in the ^{57}Fe
301 content of the RV4056 strain was measured at 5 μM heme concentrations and a 8-fold at 40
302 μM heme, by comparison with the WT (Fig. 4B).

303 To confirm the major role of the *lsa1836-1840* gene products in heme acquisition, we
304 analyzed the ^{57}Fe content of the RV4056 strain harboring the *pP_{lsa1836-1840}*, a multicopy
305 plasmid that expresses the *lsa1836-1840* operon under its own promoter, and compared it to
306 the WT. The quantification of the ^{57}Fe atoms in the RV4056 *pP_{lsa1836-1840}* bacteria shows
307 a 1.3 time and a 7 times higher iron content at 5 and 40 μM ^{57}Fe -hemin, respectively, by
308 comparison with measurements done on WT bacteria (Fig. 4C).

309 These experiments confirm that the *Lsa1836-1840* system is involved *in vitro* in the active
310 incorporation of heme in *L. sakei*.

311

312 **4. Heme accumulates inside the *L. sakei* cytosol at low heme concentrations**

313 We then addressed the ability for *L. sakei* to consume heme or iron to survive. We knew from
314 a previous study that *L. sakei* incorporates preferentially hemic-compounds from the
315 medium, probably as an adaptation to its meat environment (13). Data obtained previously
316 showed that the incorporation of heme molecules are qualitatively correlated with both the
317 concentration of heme in the growth medium, and the survival properties of the bacteria in
318 stationary phase, suggesting that *L. sakei* could use heme or iron for its survival (See
319 Supplemental text, Fig. S1 and S2). Nevertheless, heme incorporation could not be quantified
320 with accuracy in the previous studies. To tackle that, the intracellular heme levels
321 incorporated by *L. sakei* were quantified. The RV2002 *hrtR-lac* strain (Table 2) was grown in
322 MCD in the presence of increasing concentration of hemin, and the β -Gal activity of cells was
323 measured (Fig. 5A). We showed that the β -Gal activity increased with the concentration of
324 the hemin molecule in the growth medium. A plateau was reached when cells were grown in

325 0.75 - 2.5 μM hemin. Incubation of cells in higher hemin concentrations did not allow to
326 increase further β -Gal activity.

327

328 **5. Heme incorporation in *L. sakei* is rapid and massive**

329 The absolute number of heme molecules incorporated by *L. sakei* 23K (Table 2) was also
330 quantified using ^{57}Fe -hemin. Cells were grown in MCD in the presence of labeled-hemin.
331 Measurements of the ^{57}Fe content of cells showed that the incorporation of ^{57}Fe -Hemin is
332 massive and rapid as bacteria are able to incorporate about 35,000 ^{57}Fe atoms of hemic
333 origin, within 1 hour in the presence of 1 μM ^{57}Fe -Hemin (Fig. 5B). The iron content of cells
334 increased to 160,000 and 260,000 atoms in average when bacteria were grown in a medium
335 containing 5 and 40 μM of ^{57}Fe -Hemin, respectively. This indicates that the ^{57}Fe content of *L.*
336 *sakei* cells increased with the ^{57}Fe -Hemin concentration in the medium on the 1 to 40 μM
337 range. Measurements of the iron content of bacteria growing in presence of ^{57}Fe -Hemin for an
338 extended period of time (19h) did not show additional ^{57}Fe accumulation in the bacteria (Fig.
339 5B). Instead, the number of ^{57}Fe atoms associated with bacteria decreased over time
340 highlighting the fact that a massive incorporation of labeled-hemin occurs rapidly after
341 bacteria being in contact with the molecules.

342

343 **Discussion**

344 Heme acquisition systems are poorly documented in lactic acid bacteria, probably because
345 heme or iron are not mandatory for growth of these bacterial species, at least under non-
346 aerobic conditions. However, acquisition of exogenous heme allows numerous lactic acid
347 bacteria, among them *L. lactis* and *Lactobacillus plantarum*, to activate, if needed, a
348 respiratory metabolism, when grown in the presence of oxygen (2, 49, 50). This implies that
349 heme has to cross the thick cell-wall of these Gram-positive organisms and may require heme

350 transporters. Thus far, heme acquisition systems in heme auxotrophic organisms have only
351 been reported for *Streptococci* (20, 21) and *S. pyogenes*, where they both involve Shr and Shp
352 NEAT-domain proteins and Hts ABC transporter (20, 22, 23). In lactic acid bacteria, no such
353 functional heme transport has been identified so far. NEAT domains have been identified in
354 several species of lactic acid bacteria, including 15 *Lactobacillus*, 4 *Leuconostoc* and one
355 *Carnobacterium* species, but our study confirmed that *L. sakei* proteins are devoid of such
356 domains (19).

357 In *L. lactis*, the *fhuCBGDR* operon has been reported to be involved in heme uptake as a
358 *fhuD* mutant is defective in respiration metabolism, suggesting a defect in heme import (15).
359 A genome analysis of several lactic acid bacteria has revealed that a HupC/FepC heme uptake
360 protein is present in *L. lactis*, *L. plantarum*, *Lactobacillus brevis* and *L. sakei* (15). This latter
361 in *L. sakei* 23K may correspond to locus *lsa0399* included in a *fhu* operon. An IsdE homolog
362 has also been reported in *L. brevis* genome but the identity of this protein has not been
363 experimentally verified (15).

364 The genome analysis of *L. sakei* 23K (12), when focused on heme/iron transport systems and
365 heme utilization enzymes, led to the identification of several putative iron transport systems,
366 heme transport systems and heme-degrading enzymes. This heme uptake potential is
367 completely consistent within the meat environment-adapted *L. sakei*. Similarly, the membrane
368 transport system encoded by the *lsa1194-1195* genes, whose function is poorly defined,
369 seems to be important for the bacterial physiology as a *lsa1194-1195* deletion affects the
370 survival properties of this strain (see Supplemental text, Fig. S3 and Fig. S4).

371 Meanwhile, here, we report that the transcriptional unit *lsa1836-1840* shows exquisite
372 structure/function homology with the cobalamin ECF transporter, a new class of ATP-binding
373 cassette importer recently identified in the internalization of cobalt and nickel ions (Fig. 2 and
374 Fig. 3). Indeed, a comprehensive bioinformatics analysis indicates/supports that the *lsa1836-*

375 *l840* locus codes for 5 proteins that assemble together to describe a complete importer
376 machinery called Energy Coupling Factor. Any canonical ECF transporter comprises an
377 energy-coupling module consisting of a transmembrane T protein (EcfT), two nucleotide-
378 binding proteins (EcfA and EcfA'), and another transmembrane substrate-specific binding S
379 protein (Ecsf). Indeed, Lsa1836-Lsa1838 shows high structural homology with Ecf-S, EcfA-
380 A' and Ecf-T, respectively. Despite sharing similarities with ABC-transporters, ECF
381 transporters have different organizational and functional properties. The lack of soluble-
382 binding proteins in ECF transporters differentiates them clearly from the canonical ABC-
383 importers. Nevertheless here, *lsa1839* and *lsa1840* code for proteins structurally close to β
384 and α subunits of transcobalamin-binding domain, respectively. They are highly suspected to
385 be soluble proteins dedicated to scavenge heme from the extracellular compartment and we
386 hypothesize that they could bind it and then transfer it to Ecf-S component coded by *lsa1836*
387 (Fig. 3). In line with that, the heterodimer composed of Lsa1839 & Lsa1840, possibly β and
388 α subunits, respectively, have been modeled *in silico* and were shown to accommodate with
389 high affinity an iron-heme ligand at the binding site located at the interface of the two
390 proteins.

391 Internalization of the cobalt and nickel divalent cations through porphyrin moiety *via* this new
392 class of importer has been demonstrated in lactic acid bacteria, such as *L. lactis* and *L. brevis*.
393 However, nothing was known for the internalization/incorporation of iron-containing heme. A
394 functional analysis of the *lsa1836-1840* gene products was undertaken using Δ *lsa1836-1840*
395 deletion mutant and a complemented strain. Our experiments indicate that the intracellular
396 abundance of heme is significantly reduced in Δ *lsa1836-1840* mutant bacterial cells at 1 and 5
397 μ M heme, while it is similar to the WT at low heme concentrations. Reversely, the mutant
398 strain in which *lsa1836-1840* is expressed from a multicopy plasmid, showed an increase in
399 the heme uptake. Taken together, these experiments confirm that the Lsa1836-1840 system is

400 involved *in vitro* in the active incorporation of heme in *L. sakei*. Also, our synteny analysis
401 for this operon shows that this feature could be shared within several Gram-positive meat-
402 borne bacteria.

403 Additionally, we were able to quantify the amount of heme internalized in the three genetic
404 contexts using isotope-labeled hemin and ICP-MS as well as to evaluate the intracellular
405 content of heme using the transcriptional fusion tool. We observed that the intracellular
406 abundance of heme increases with the concentration of heme in the growth medium and can
407 be detected with the intracellular sensor in the 0 - 2.5 μM heme range (Fig. 5A). The drop in
408 the β -gal activity at higher heme concentrations may result from regulation of heme/iron
409 homeostasis either through exportation of heme, degradation of the intracellular heme or
410 storage of the heme molecules, making them unable to interact with HrtR and promoting *lacZ*
411 repression. However, data obtained with the intracellular sensor at higher heme concentration
412 (5-40 μM) contrast with microscopic observations (Fig. S2) and ICP-MS measurements (Fig.
413 5B) that reported a higher hemic-iron content in cells grown in 40 μM heme than in 5 μM .
414 Indeed, β -gal activity reflecting the abundance of intracellular heme was maximal when cells
415 were grown in a medium containing 1-2.5 μM hemin (Fig. 5A), while ICP-MS measurements
416 showed a 4.5 fold and 8 fold higher number of ^{57}Fe atoms in bacteria growing in 5 μM or 40
417 μM ^{57}Fe -Hemin, respectively, than in 1 μM ^{57}Fe -Hemin (Fig. 4B). These data are in good
418 agreement with EELS analysis (Fig. S2), which strengthens the hypothesis that heme
419 homeostasis occurs in *L. sakei* and that the incorporated heme molecules would be degraded
420 while iron is stored inside iron storage proteins like Dps, of which orthologous genes exist in
421 *L. sakei*. Thus iron is detected in *L. sakei* cells but not bound to heme and unable to interact
422 with the intracellular heme sensor HrtR. Storage of heme inside membrane proteins is still an
423 open question as *L. sakei* does not contain cytochromes nor menaquinones (12).

424

425 Further analysis is required not only to decipher the exact role of these proteins during the
426 different steps of heme transport across the *L. sakei* membrane and the fate of heme inside *L.*
427 *sakei* cells, but also to understand the molecular specificity of the Lsa1836-1840 machinery
428 towards iron-containing heme *versus* cobalamin.

429

430 **Materials and methods**

431

432 **Bacterial strains and general growth conditions.**

433 The different bacterial strains used throughout this study are described in Table 1.
434 *Lactobacillus sakei* and its derivatives (RV2002 RV2002 hrtR-lac RV4056 RV4056c
435 RV4057 RV4057 hrtR-lac) were propagated on MRS (2) at 30°C. For physiological studies
436 the chemically defined medium MCD (3) supplemented with 0.5% (wt/vol) glucose was used.
437 MCD contains no iron sources but contains possible traces of iron coming from various
438 components or distilled water. Incubation was performed at 30°C without stirring. Cell
439 growth and viability of cells in stationary phase were followed by measuring the optical
440 density at 600 nm (OD₆₀₀) on a visible spectrophotometer (Secoman) and by the
441 determination of the number of CFU ml⁻¹ after plating serial dilutions of samples on MRS
442 agar. When needed, media were supplemented with filtered hemin or hematin (Sigma-
443 Aldrich) or with ⁵⁷Fe-hemin (Frontier Scientific) solutions resuspended in 50 mM NaOH.
444 *Escherichia coli* K-12 strain DH5α was used as the host for plasmid construction and cloning
445 experiments. *E. coli* cells were chemically transformed as previously described (4). *L. sakei*
446 cells were transformed by electroporation as previously described (5). For routine growth, *E.*
447 *coli* strain was propagated in LB at 37°C under vigorous shaking (175 rpm). The following
448 concentrations of antibiotic were used for bacterial selection: kanamycin at 20 µg/mL and
449 ampicillin at 100 µg/mL for *E. coli* and erythromycin at 5 µg/mL for *L. sakei*.

450

451 **DNA manipulations.**

452 Chromosomal DNA was extracted from *Ls* cells with DNA Isolation Kit for Cells and Tissues
453 (Roche, France). Plasmid DNA was extracted from *E. coli* by a standard alkaline lysis
454 procedure with NucleoSpin® Plasmid Kit (Macherey Nagel, France). PCR-amplified
455 fragments and digested fragments separated on 0.8% agarose gels were purified with kits
456 from Qiagen (France). Restriction enzymes, *Taq* or *Phusion* high-fidelity polymerase
457 (ThermoScientific, France) and T4 DNA ligase (Roche) were used in accordance with the
458 manufacturer's recommendations. Oligonucleotides (Table 3) were synthesized by
459 Eurogentec (Belgium). PCRs were performed in Applied Biosystems 2720 Thermak
460 thermocycler (ABI). Nucleotide sequences of all constructs were determined by MWG -
461 Eurofins (Germany).

462

463 **Bioinformatic analyses**

464 Analyses were performed in the sequenced *L. sakei* 23K genome as described in (12). Each
465 fasta sequence of every gene of the operon comprised between *lsa1836* and *lsa1840* was
466 retrieved from UniProtKB server at <http://www.uniprot.org/uniprot>, uploaded then analyzed
467 using HHpred server (44) that detects structural homologues. For *Lsa1839* and *Lsa1840*, that
468 partly shares strong structural homology with Geranyl-geranyltransferase type-I (pdb id 5nsa,
469 chain A) (51), and β domain of human haptocorrin (pdb id 4kki chain A) (52), intrinsic factor
470 with cobalamin (pdb id 2pmv) (53) and transcobalamin (pdb id 2bb6 chainA) (54)
471 respectively, homology modeling was performed using Modeller, version Mod9v18 (55). The
472 heterodimer was then formed with respect to the functional and structural assembly of α and
473 β domains of the native haptocorrin (52). Upon dimer formation, the best poses for heme
474 within the groove, located at the interface of this heterodimer, were computed using

475 Autodock4 tool (56). The protocol and grid box were previously validated with the redocking
476 of cyanocobalamin within human haptocorrin (4kki) (42) and of cobalamin within bovine
477 transcobalamin (2bb6). To compute the binding energy of every complex, the parameters of
478 the cobalt present in the cobalamin and cyanocobalamin were added to the parameter data
479 table, the iron parameters of the heme are already in the parameter data table. Then the
480 docking poses were explored using the Lamarckian genetic algorithm. The poses of the
481 ligands were subsequently analyzed with PyMOL of the Schrödinger suite (57).
482 Comparative genomic analysis for conservation of gene synteny between meat-borne bacteria
483 was carried out with the MicroScope Genome Annotation platform, using the Genome
484 Synteny graphical output and the PkGDB Synteny Statistics (58)

485

486 **Construction of plasmids and *L. sakei* mutant strains.**

487 All the primers and plasmids used in this study are listed in Table 2 and 3. The *lsa1836-1840*
488 genes were inactivated by a 5118 bp deletion using double cross-over strategy. Upstream and
489 downstream fragments were obtained using primers pairs PHDU-*lsa1836F*/PHDU-*lsa1836R*
490 (731 bp) and PHDU-*lsa1840F*/PHDU-*lsa1840R* (742 bp) (Table 3). PCR fragments were
491 joined by SOE using primers PHDU-*lsa1836F*/PHDU-*lsa1840R* and the resulting 1456 bp
492 fragment was cloned between *EcoRI* and *KpnII* sites in pRV300 yielding the pRV441 (Table
493 2). pRV441 was introduced in the *L. sakei* 23K and the *L. sakei* 23K Δ *lacLM* (RV2002)
494 strains by electroporation as described previously (59). Selection was done on erythromycin
495 sensitivity. Second cross-over erythromycin sensitive candidates were screened using primers
496 PHDU-*crblsa1840F* and PHDU-*crblsa1840R* (Table 3). Deletion was then confirmed by
497 sequencing the concerned region and the *lsa1836-1840* mutant strains were named RV4056
498 and RV4057 (Table 2).

499 To construct the RV2002 *hrtR-lac* and the RV4057 *hrtR-lac* strains, the pP_{*hrt*}*hrtR-lac* (Table

500 2) was transformed by electroporation into the corresponding mother strains.
501 For complementation, a *pP_{lsa1836-1840}* plasmid (Table 2) was constructed as follows: a
502 DNA fragment encompassing the promoter and the 5 genes of the *lsa1836-1840* operon was
503 PCR amplified using the primers pair Lsa1836R/Lsa1840F (Table 3). The 5793 bp amplified
504 fragment was cloned into plasmid pRV566 at *Xma*I and *Not*I sites. The construct was verified
505 by sequencing the whole DNA insert using the 566-F and 566-R primers (Table 3) as well as
506 internal primers. The *pP_{lsa1836-1840}* was introduced into RV4056 bacteria by
507 electroporation and transformed bacteria were selected for erythromycin resistance, yielding
508 the RV4056c complemented mutant strain.

509

510 **β -galactosidase assay**

511 Liquid cultures were usually grown in MCD into exponentially phase corresponding to a A_{600}
512 equal to 0,5-0.8 and then incubated for 1 h at 30°C with hemin at the indicated concentration.
513 β -Galactosidase (β -Gal) activity was assayed on bacteria permeabilized as described. β -Gal
514 activity was quantified by luminescence in an Infinite M200 spectroluminometer (Tecan)
515 using the β -Glo® assay system as recommended by manufacturer (Promega).

516

517 **Intracellular iron ^{57}Fe determination**

518 The various strains were grown in MCD to $A_{600} = 0.5-0.7$ at 30°C prior to addition or not of
519 0.1, 1, 5 or 40 μM ^{57}Fe -labelled hemin (Frontier Scientific). Cells were then incubated at
520 30°C for an additional hour and overnight (19 hours). Cells were washed three times in H_2O
521 supplemented with 1mM EDTA. Cell pellets were desiccated and mineralized by successive
522 incubations in 65% nitric acid solution at 130°C. ^{57}Fe was quantified by Inductively Coupled
523 Plasma Mass Spectroscopy (ICP-MS) (Agilent 7700X), Géosciences, University of
524 Montpellier (France).

525

526 **Acknowledgments**

527 This work, including Emilie Verplaetse post-doctoral grant, was funded from the French
528 National Research Agency ANR-11-IDEX-0003-02; ‘ALIAS’ project.

529 The authors would like to thank Véronique Martin for her help in setting up the cobalt
530 parameter in the Autodock table parameter, Elise Abi-Khalil for the construction of the
531 pLsa1836-1840, Delphine Lechardeur and Alexandra Gruss for the heme reporter plasmid and
532 fruitful discussion and support.

533

534

535 **References**

- 536 1. Neilands JB. 1981. Microbial Iron Compounds. *Annu Rev Biochem* 50:715–731.
- 537 2. Brooijmans R, Smit B, Santos F, van Riel J, de Vos WM, Hugenholtz J. 2009. Heme
538 and menaquinone induced electron transport in lactic acid bacteria. *Microb Cell Factories*
539 8:28.
- 540 3. Pandey A, Bringel F, Meyer J-M. 1994. Iron requirement and search for siderophores
541 in lactic acid bacteria. *Appl Microbiol Biotechnol* 40:735–739.
- 542 4. Champomier MC, Montel MC, Grimont F, Grimont PA. 1987. Genomic identification
543 of meat *Lactobacilli* as *Lactobacillus sake*. *Ann Inst Pasteur Microbiol* 138:751–758.
- 544 5. Bredholt S, Nesbakken T, Holck A. 1999. Protective cultures inhibit growth of
545 *Listeria monocytogenes* and *Escherichia coli* O157:H7 in cooked, sliced, vacuum- and gas-
546 packaged meat. *Int J Food Microbiol* 53:43–52.
- 547 6. Leroy F, Lievens K, De Vuyst L. 2005. Modeling Bacteriocin Resistance and
548 Inactivation of *Listeria innocua* LMG 13568 by *Lactobacillus sakei* CTC 494 under Sausage
549 Fermentation Conditions. *Appl Environ Microbiol* 71:7567–7570.
- 550 7. Vermeiren L, Devlieghere F, Debevere J. 2004. Evaluation of meat born lactic acid
551 bacteria as protective cultures for the biopreservation of cooked meat products. *Int J Food*
552 *Microbiol* 96:149–164.
- 553 8. Chaillou S, Christieans S, Rivollier M, Lucquin I, Champomier-Vergès MC, Zagorec
554 M. 2014. Quantification and efficiency of *Lactobacillus sakei* strain mixtures used as
555 protective cultures in ground beef. *Meat Sci* 97:332–338.
- 556 9. Devlieghere F, Francois K, Vereecken KM, Geeraerd AH, Van Impe JF, Debevere J.
557 2004. Effect of chemicals on the microbial evolution in foods. *J Food Prot* 67:1977–1990.
- 558 10. Lombardi-Boccia G, Martinez-Dominguez B, Aguzzi A. 2002. Total Heme and Non-
559 heme Iron in Raw and Cooked Meats. *J Food Sci* 67:1738–1741.

- 560 11. Hertel C, Schmidt G, Fischer M, Oellers K, Hammes WP. 1998. Oxygen-Dependent
561 Regulation of the Expression of the Catalase Gene *katA* of *Lactobacillus sakei* LTH677. *Appl*
562 *Environ Microbiol* 64:1359–1365.
- 563 12. Chaillou S, Champomier-Vergès M-C, Cornet M, Crutz-Le Coq A-M, Dudez A-M,
564 Martin V, Beauvils S, Darbon-Rongère E, Bossy R, Loux V, Zagorec M. 2005. The complete
565 genome sequence of the meat-borne lactic acid bacterium *Lactobacillus sakei* 23K. *Nat*
566 *Biotechnol* 23:1527–1533.
- 567 13. Duhutrel P, Bordat C, Wu T-D, Zagorec M, Guerquin-Kern J-L, Champomier-Verges
568 M-C. 2010. Iron Sources Used by the Nonpathogenic Lactic Acid Bacterium *Lactobacillus*
569 *sakei* as Revealed by Electron Energy Loss Spectroscopy and Secondary-Ion Mass
570 Spectrometry. *Appl Environ Microbiol* 76:560–565.
- 571 14. Huang W, Wilks A. 2017. Extracellular Heme Uptake and the Challenge of Bacterial
572 Cell Membranes. *Annu Rev Biochem* 86:799–823.
- 573 15. Gruss A, Borezée-Durant E, Lechardeur D. 2012. Chapter Three - Environmental
574 Heme Utilization by Heme-Auxotrophic Bacteria, p. 69–124. *In* Robert K. Poole (ed.),
575 *Advances in Microbial Physiology*. Academic Press.
- 576 16. Choby JE, Skaar EP. 2016. Heme Synthesis and Acquisition in Bacterial Pathogens. *J*
577 *Mol Biol* 428:3408–3428.
- 578 17. Anzaldi LL, Skaar EP. 2010. Overcoming the Heme Paradox: Heme Toxicity and
579 Tolerance in Bacterial Pathogens. *Infect Immun* 78:4977–4989.
- 580 18. Reniere ML, Torres VJ, Skaar EP. 2007. Intracellular metalloporphyrin metabolism in
581 *Staphylococcus aureus*. *BioMetals* 20:333–345.
- 582 19. Honsa ES, Maresso AW, Highlander SK. 2014. Molecular and Evolutionary Analysis
583 of NEAr-Iron Transporter (NEAT) Domains. *PLoS ONE* 9:e104794.
- 584 20. Bates CS, Montanez GE, Woods CR, Vincent RM, Eichenbaum Z. 2003.

- 585 Identification and Characterization of a *Streptococcus pyogenes* Operon Involved in Binding
586 of Hemoproteins and Acquisition of Iron. *Infect Immun* 71:1042–1055.
- 587 21. Meehan M, Burke FM, Macken S, Owen P. 2010. Characterization of the haem-uptake
588 system of the equine pathogen *Streptococcus equi subsp. equi*. *Microbiology* 156:1824–1835.
- 589 22. Lei B, Smoot LM, Menning HM, Voyich JM, Kala SV, Deleo FR, Reid SD, Musser
590 JM. 2002. Identification and Characterization of a Novel Heme-Associated Cell Surface
591 Protein Made by *Streptococcus pyogenes*. *Infect Immun* 70:4494–4500.
- 592 23. Ouattara M, Bentley Cunha E, Li X, Huang Y-S, Dixon D, Eichenbaum Z. 2010. Shr
593 of group A *streptococcus* is a new type of composite NEAT protein involved in sequestering
594 haem from methaemoglobin: Haem uptake and reduction by Shr. *Mol Microbiol* 78:739–756.
- 595 24. Lechardeur D, Cesselin B, Liebl U, Vos MH, Fernandez A, Brun C, Gruss A, Gaudu
596 P. 2012. Discovery of Intracellular Heme-binding Protein HrtR, Which Controls Heme Efflux
597 by the Conserved HrtB-HrtA Transporter in *Lactococcus lactis*. *J Biol Chem* 287:4752–4758.
- 598 25. Joubert L, Derré-Bobillot A, Gaudu P, Gruss A, Lechardeur D. 2014. HrtBA and
599 menaquinones control haem homeostasis in *Lactococcus lactis*: Membrane and intracellular
600 haem control in *Lactococcus lactis*. *Mol Microbiol* 93:823–833.
- 601 26. Rempel S, Stanek WK, Slotboom DJ. 2019. ECF-Type ATP-Binding Cassette
602 Transporters. *Annu Rev Biochem* 88:551–576.
- 603 27. Finkenwirth F, Eitinger T. 2019. ECF-type ABC transporters for uptake of vitamins
604 and transition metal ions into prokaryotic cells. *Res Microbiol*.
- 605 28. Wang T, Fu G, Pan X, Wu J, Gong X, Wang J, Shi Y. 2013. Structure of a bacterial
606 energy-coupling factor transporter. *Nature* 497:272–276.
- 607 29. Bao Z, Qi X, Hong S, Xu K, He F, Zhang M, Chen J, Chao D, Zhao W, Li D, Wang J,
608 Zhang P. 2017. Structure and mechanism of a group-I cobalt energy coupling factor
609 transporter. *Cell Res* 27:675–687.

- 610 30. Zhang M, Bao Z, Zhao Q, Guo H, Xu K, Wang C, Zhang P. 2014. Structure of a
611 pantothenate transporter and implications for ECF module sharing and energy coupling of
612 group II ECF transporters. *Proc Natl Acad Sci U S A* 111:18560–18565.
- 613 31. Xu K, Zhang M, Zhao Q, Yu F, Guo H, Wang C, He F, Ding J, Zhang P. 2013. Crystal
614 structure of a folate energy-coupling factor transporter from *Lactobacillus brevis*. *Nature*
615 497:268–271.
- 616 32. Rodionov DA, Hebbeln P, Eudes A, ter Beek J, Rodionova IA, Erkens GB, Slotboom
617 DJ, Gelfand MS, Osterman AL, Hanson AD, Eitinger T. 2009. A novel class of modular
618 transporters for vitamins in prokaryotes. *J Bacteriol* 191:42–51.
- 619 33. Henderson GB, Zevely EM, Huennekens FM. 1979. Mechanism of folate transport in
620 *Lactobacillus casei*: evidence for a component shared with the thiamine and biotin transport
621 systems. *J Bacteriol* 137:1308–1314.
- 622 34. Burgess CM, Slotboom DJ, Geertsma ER, Duurkens RH, Poolman B, van Sinderen D.
623 2006. The riboflavin transporter RibU in *Lactococcus lactis*: molecular characterization of
624 gene expression and the transport mechanism. *J Bacteriol* 188:2752–2760.
- 625 35. Turner MS, Tan YP, Giffard PM. 2007. Inactivation of an Iron Transporter in
626 *Lactococcus lactis* Results in Resistance to Tellurite and Oxidative Stress. *Appl Environ*
627 *Microbiol* 73:6144–6149.
- 628 36. Li L, Chen OS, Ward DM, Kaplan J. 2001. CCC1 Is a Transporter That Mediates
629 Vacuolar Iron Storage in Yeast. *J Biol Chem* 276:29515–29519.
- 630 37. Fernandez A, Lechardeur D, Derré-Bobillot A, Couvé E, Gaudu P, Gruss A. 2010.
631 Two Coregulated Efflux Transporters Modulate Intracellular Heme and Protoporphyrin IX
632 Availability in *Streptococcus agalactiae*. *PLoS Pathog* 6:e1000860.
- 633 38. von Heijne G. 1992. Membrane protein structure prediction. Hydrophobicity analysis
634 and the positive-inside rule. *J Mol Biol* 225:487–494.

- 635 39. Jin B, Newton SMC, Shao Y, Jiang X, Charbit A, Klebba PE. 2006. Iron acquisition
636 systems for ferric hydroxamates, haemin and haemoglobin in *Listeria monocytogenes*. *Mol*
637 *Microbiol* 59:1185–1198.
- 638 40. Abi-Khalil E, Segond D, Terpstra T, Andre-Leroux G, Kallassy M, Lereclus D, Bou-
639 Abdallah F, Nielsen-Leroux C. 2015. Heme interplay between IIsA and IsdC: Two
640 structurally different surface proteins from *Bacillus cereus*. *Biochim Biophys Acta*
641 1850:1930–1941.
- 642 41. Maresso AW, Chapa TJ, Schneewind O. 2006. Surface Protein IsdC and Sortase B
643 Are Required for Heme-Iron Scavenging of *Bacillus anthracis*. *J Bacteriol* 188:8145–8152.
- 644 42. Mazmanian SK, Skaar EP, Gaspar AH, Humayun M, Gornicki P, Jelenska J,
645 Joachmiak A, Missiakas DM, Schneewind O. 2003. Passage of heme-iron across the envelope
646 of *Staphylococcus aureus*. *Science* 299:906–909.
- 647 43. Mazmanian SK, Ton-That H, Su K, Schneewind O. 2002. An iron-regulated sortase
648 anchors a class of surface protein during *Staphylococcus aureus* pathogenesis. *Proc Natl Acad*
649 *Sci* 99:2293–2298.
- 650 44. Söding J, Biegert A, Lupas AN. 2005. The HHpred interactive server for protein
651 homology detection and structure prediction. *Nucleic Acids Res* 33:W244-248.
- 652 45. Szklarczyk D, Gable AL, Lyon D, Junge A, Wyder S, Huerta-Cepas J, Simonovic M,
653 Doncheva NT, Morris JH, Bork P, Jensen LJ, Mering C von. 2019. STRING v11: protein–
654 protein association networks with increased coverage, supporting functional discovery in
655 genome-wide experimental datasets. *Nucleic Acids Res* 47:D607–D613.
- 656 46. Roberts JN, Singh R, Grigg JC, Murphy MEP, Bugg TDH, Eltis LD. 2011.
657 Characterization of Dye-Decolorizing Peroxidases from *Rhodococcus jostii* RHA1.
658 *Biochemistry* 50:5108–5119.
- 659 47. Singh R, Grigg JC, Armstrong Z, Murphy MEP, Eltis LD. 2012. Distal Heme Pocket

- 660 Residues of B-type Dye-decolorizing Peroxidase: ARGININE BUT NOT ASPARTATE IS
661 ESSENTIAL FOR PEROXIDASE ACTIVITY. *J Biol Chem* 287:10623–10630.
- 662 48. Lauret R, Morel-Deville F, Berthier F, Champomier-Verges M, Postma P, Ehrlich SD,
663 Zagorec M. 1996. Carbohydrate utilization in *Lactobacillus sake*. *Appl Environ Microbiol*
664 62:1922–1927.
- 665 49. Gaudu P, Vido K, Cesselin B, Kulakauskas S, Tremblay J, Rezaiki L, Lamberret G,
666 Sourice S, Duwat P, Gruss A. 2002. Respiration capacity and consequences in *Lactococcus*
667 *lactis*. *Antonie Van Leeuwenhoek* 82:263–269.
- 668 50. Lechardeur D, Cesselin B, Fernandez A, Lamberet G, Garrigues C, Pedersen M,
669 Gaudu P, Gruss A. 2011. Using heme as an energy boost for lactic acid bacteria. *Curr Opin*
670 *Biotechnol* 22:143–149.
- 671 51. Bloch JS, Ruetz M, Kräutler B, Locher KP. 2017. Structure of the human
672 transcobalamin beta domain in four distinct states. *PLOS ONE* 12:e0184932.
- 673 52. Furger E, Frei DC, Schibli R, Fischer E, Prota AE. 2013. Structural Basis for
674 Universal Corrinoid Recognition by the Cobalamin Transport Protein Haptocorrin. *J Biol*
675 *Chem* 288:25466–25476.
- 676 53. Mathews FS, Gordon MM, Chen Z, Rajashankar KR, Ealick SE, Alpers DH, Sukumar
677 N. 2007. Crystal structure of human intrinsic factor: Cobalamin complex at 2.6-Å resolution.
678 *Proc Natl Acad Sci* 104:17311–17316.
- 679 54. Wuerges J, Garau G, Geremia S, Fedosov SN, Petersen TE, Randaccio L. 2006.
680 Structural basis for mammalian vitamin B12 transport by transcobalamin. *Proc Natl Acad Sci*
681 103:4386–4391.
- 682 55. Webb B, Sali A. 2016. Comparative Protein Structure Modeling Using MODELLER.
683 *Curr Protoc Bioinforma* 54:5.6.1-5.6.37.
- 684 56. Morris GM, Goodsell DS, Halliday RS, Huey R, Hart WE, Belew RK, Olson AJ.

- 685 1998. Automated docking using a Lamarckian genetic algorithm and an empirical binding
686 free energy function. *J Comput Chem* 19:1639–1662.
- 687 57. The PyMOL Molecular Graphics System, Version 2.0. Schrödinger, LLC.
- 688 58. Vallenet D, Belda E, Calteau A, Cruveiller S, Engelen S, Lajus A, Le Fèvre F, Longin
689 C, Mornico D, Roche D, Rouy Z, Salvignol G, Scarpelli C, Thil Smith AA, Weiman M,
690 Médigue C. 2013. MicroScope—an integrated microbial resource for the curation and
691 comparative analysis of genomic and metabolic data. *Nucleic Acids Res* 41:D636–D647.
- 692 59. Berthier F, Zagorec M, Champomier-Verges M, Ehrlich SD, Morel-Deville F. 1996.
693 Efficient transformation of *Lactobacillus sakei* by electroporation. *Microbiology* 142:1273–
694 1279.
- 695 60. Stentz R, Loizel C, Malleret C, Zagorec M. 2000. Development of Genetic Tools for
696 *Lactobacillus sakei*: Disruption of the β -Galactosidase Gene and Use of *lacZ* as a Reporter
697 Gene To Study Regulation of the Putative Copper ATPase, *AtkB*. *Appl Environ Microbiol*
698 66:4272–4278.
- 699 61. Leloup L, Ehrlich SD, Zagorec M, Morel-Deville F. 1997. Single-crossover
700 integration in the *Lactobacillus sakei* chromosome and insertional inactivation of the *ptsI* and
701 *lacL* genes. *Appl Environ Microbiol* 63:2117–2123.
- 702 62. Alpert C-A, Crutz-Le Coq A-M, Malleret C, Zagorec M. 2003. Characterization of a
703 Theta-Type Plasmid from *Lactobacillus sakei*: a Potential Basis for Low-Copy-Number
704 Vectors in *Lactobacilli*. *Appl Environ Microbiol* 69:5574–5584.

705

706

707

708

709

710 **Table 1**

Locus tag and Functional category	Predicted protein function
ABC transporters	
<i>lsa0399-0402</i>	Fhu
<i>lsa1836-1840</i>	Putative metal ion ABC transporter, cobalamin transporter
<i>lsa1366-1367</i>	Putative ABC exporter (heme-efflux machinery)
Proton-motive force transporters	
<i>lsa0246</i>	Mn ²⁺ / Zn ²⁺ / Fe ²⁺ transporter
<i>lsa1699</i>	Mn ²⁺ / Zn ²⁺ / Fe ²⁺ transporter
Membrane proteins	
<i>lsa1194-1195</i>	Uncharacterized proteins
Heme-modifying enzyme	
<i>lsa1831</i>	Dyp-type peroxidase

711

712

713 **Table 2:** Strains and plasmids used in this study

714

Strains or plasmids	Characteristics	References
Strains		
<i>Lactobacillus sakei</i> 23K	sequenced strain	(12)
RV2002	23K derivative, $\Delta lacLM$	(60)
RV2002 hrtR-lac	RV2002 carrying the $pP_{hrt} hrtR-lac$, ery^R	This study
RV4056	23K derivative, $\Delta isa1836-1840$	This study
RV4056c	RV4056 carrying the $pP_{isa1836-1840}$, ery^R	This study
RV4057	RV2002 $\Delta isa1836-1840$	This study
RV4057 hrtR-lac	RV4057 carrying the $pP_{hrt} hrtR-lac$, ery^R	This study
Plasmids		
$pP_{hrt} hrtR-lac$	Plasmid carrying the $P_{hrt} hrtR-lac$ transcriptional fusion	(24)
pRV300	Shuttle vector, non-replicative in <i>Lactobacillus</i> ; Amp^R , Erm^R	(61)
pRV566	vector used for complementation; Amp^R , Erm^R	(62)
pRV441	pRV300 derivative, exchange cassette for <i>isa1836-1840</i>	This study
pP _{isa1836-1840}	pRV566 carrying the promoter and the <i>isa1836-1840</i> coding sequences	This study

715

716

717

718

719

720

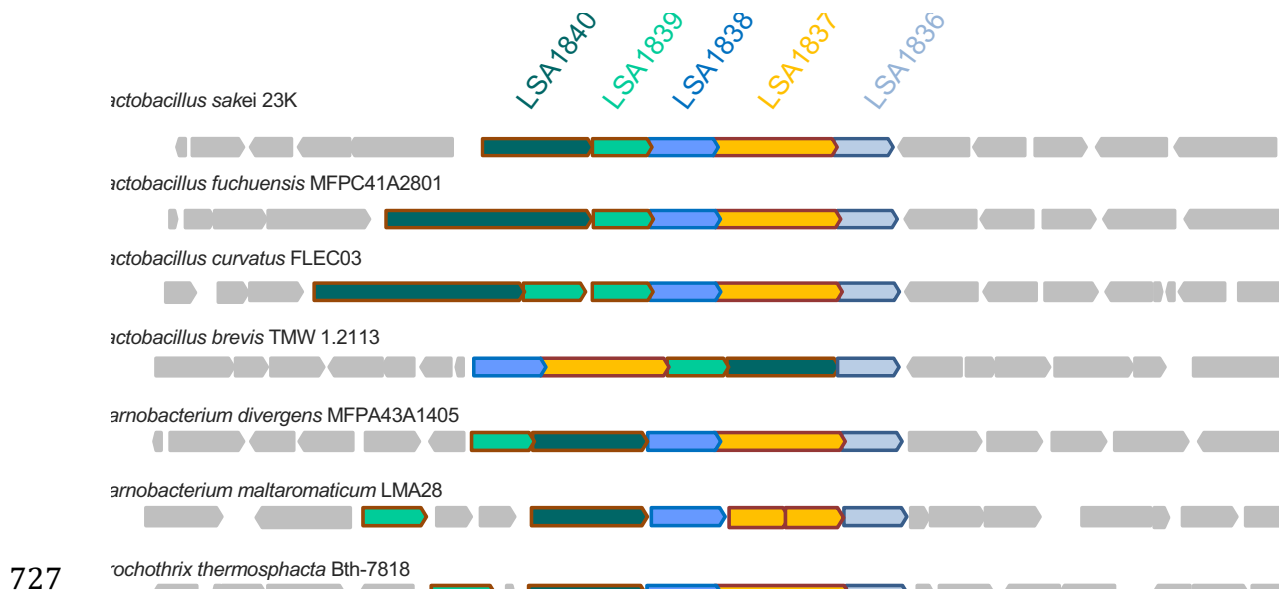
721 **Table 3:** Oligonucleotides used in this study

Primer	Sequence ^a (5'-3')	Restriction site
PHDU-<i>lsa</i>1836F	CAT <u>GGTACCGG</u> TCCGGCTCAATTATGAGT	<i>KpnI</i>
PHDU-<i>lsa</i>1836R	AATGAACTAGTTAGCGCTCGCAGCCTATATTGCGAGT	
PHDU-<i>lsa</i>1840F	AGCGCTAACTAGTTCATTAGACTTCCGTCACTTGTGAA	
PHDU-<i>lsa</i>1840R	CTGGAATTCATGCTGAGCGATGGTTTCT	<i>EcoRI</i>
PHDU-<i>crblsa</i>1840F	CGACAAGTCAACTCAGTGCTA	
PHDU-<i>crblsa</i>1840R	GTGAACCGTAATCTTGAGTG	
Lsa1836R	TTCCCGGGA <u>ACTTACAAA</u> AGGCCACGC	<i>XmaI</i>
Lsa1840F	AAAAGCGGCCGCGCCTCCTTATAAAAACTG	<i>NotI</i>
566-F	GCGAAAGAATGATGTGTTGG	
566-R	CACACAGGAAACAGCTATGAC	

722

723 ^a underlined sequences indicate the location of restriction sites, and italicized letters indicate
724 complementary overlapping sequences used to join PCR fragments as described in the
725 material and methods section.

726



727

728

729 Figure 1: Gene synteny within and around the *lsa1836-1840* gene cluster of *L. sakei* 23K with

730 other Gram-positive species found frequently on meat products. Genes in grey background

731 are unrelated to this cluster and are not conserved between the different genomes. The name

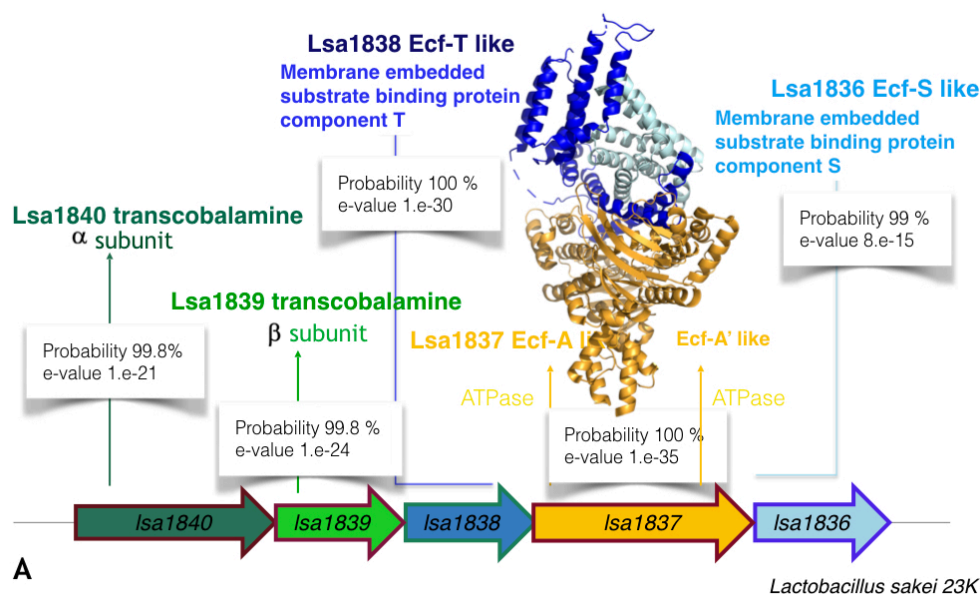
732 of the species and of the strains used for analysis are depicted on the right. All of this species

733 contains a *kata* gene (encoding a heme-dependent catalase) in their genome. Other meat-

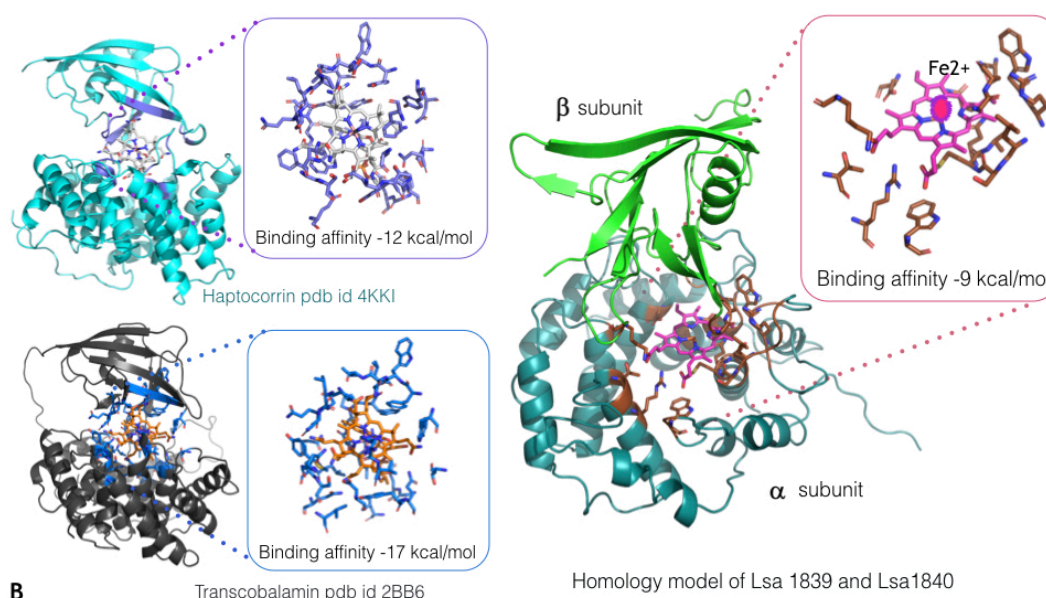
734 borne species including *Leuconostoc*, *Lactococcus*, *Vagococcus* species also found on meat

735 are not shown due to the lack of both *kata* gene and *lsa1836-1840* gene cluster.

736



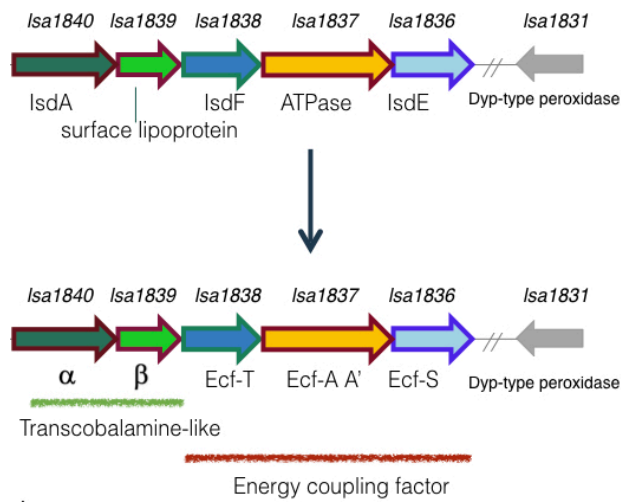
737



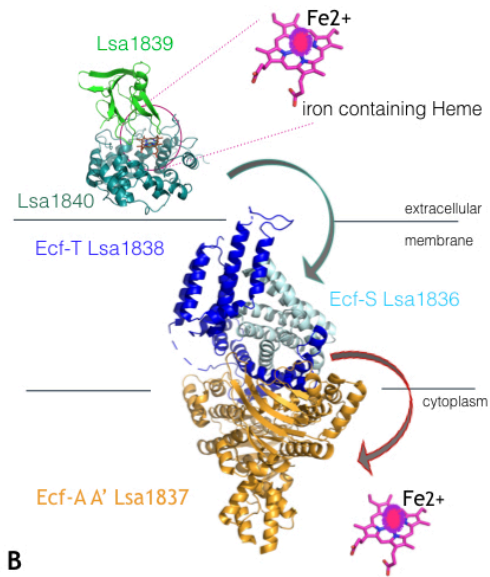
738

739 Figure 2: Panel A details the structural and functional bioinformatic assessment for each gene
740 of the *lsa1836-1840* operon. Panel B focuses on Lsa1839 and Lsa1840 and highlights (left)
741 the binding interaction and affinity of the human haptocorrin with cyano-cobalamin and
742 bovine transcobalamin with cobalamin, respectively. They were used as 3D template and
743 positive control for the modeling of transcobalamin-like proteins Lsa1840 and Lsa1839. Panel
744 B (right) shows the best pose of iron containing heme as computed by Autodock4 within the
745 binding pocket formed at the interface of a and b subunits of homology modeled Lsa1840 and
746 Lsa1839, respectively.

Functional reannotation of the operon



Heme cargoed from outside to inside



747 A

748

749 Figure 3: A, Functional reannotation of the operon *lsa1836-1840* from *L. sakei* 23K after

750 serial analysis of 3D structure/function prediction for each gene of the operon. B,

751 Reconstitution of iron-containing heme transport, initially scavenged between the a and b

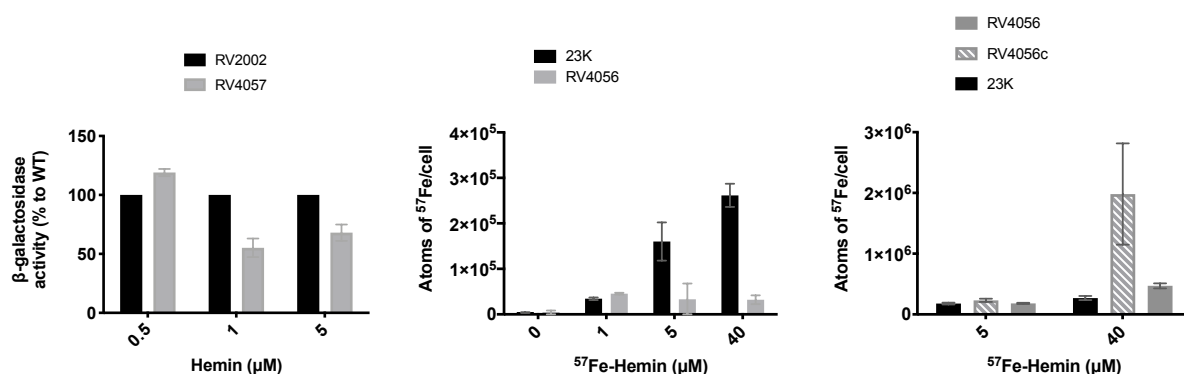
752 subunits of the transcobalamine-like transporter, coded by *lsa1839-1840*, then cargoed from

753 the extracellular into the intracellular compartments through the complete ECF machinery

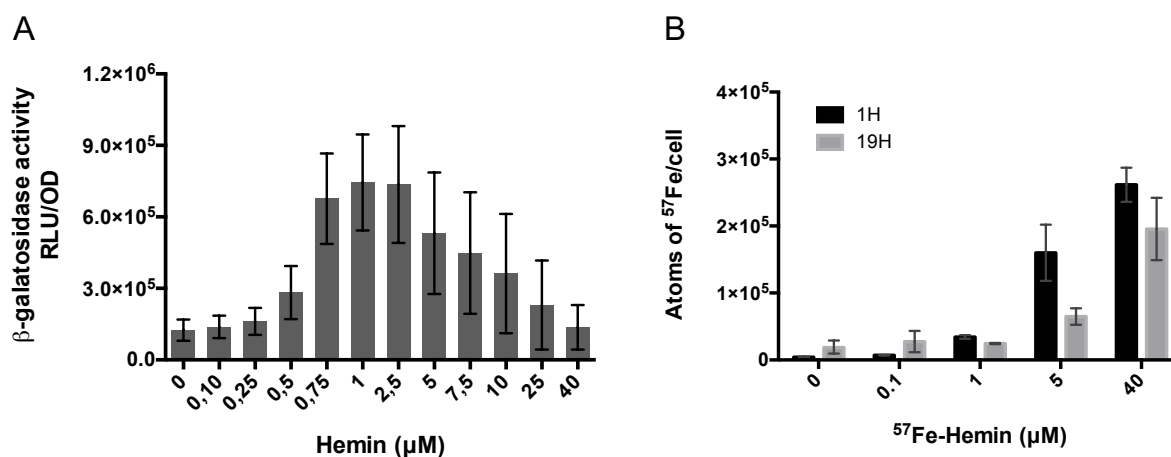
754 coded by *lsa1836-1838* portion of the operon. Possibly, gene *lsa1831* positioned in the

755 vicinity of the loci *lsa1836-1840* could code for a protein Dyp-type peroxidase that ultimately

756 releases the iron from the heme.



757
 758
 759 Figure 4: Heme incorporation is reduced in the $\Delta lsa1836-1840$ *L. sakei* deletion mutant. A, *In*
 760 *vivo* detection of intracellular heme content of the RV2002 and $\Delta lsa1836-1840$ (RV4057)
 761 mutant strains. Strains carrying the $pP_{hrtR}hrfR-lac$ were grown in hemin and β -Gal activity
 762 was quantified by luminescence (see “Material and methods”). For each experiment, values of
 763 luminescence obtained with no added hemin are subtracted and β -Gal activity of strains was
 764 expressed as the percentage to the RV2002 strain for each hemin concentration. Mean values
 765 are shown (n=3). Error bars represent the standard deviation. B, Quantification of the ⁵⁷Fe
 766 content of the WT (23K) and the $\Delta lsa1836-1840$ (RV4056) strains grown in the absence and
 767 presence of indicated ⁵⁷Fe-hemin concentrations. Results represent the mean and range from
 768 at least two independent experiments. C, Quantification of the ⁵⁷Fe content of the WT (23K),
 769 the $\Delta lsa1836-1840$ (RV4056) and the $\Delta lsa1836-1840$ $pPlsa1836-1840$ (RV4056c) strains
 770 grown in the absence and presence of indicated ⁵⁷Fe-hemin concentrations. Results represent
 771 the mean and range of two independent experiments.



772

773

774 Figure 5: Quantification of heme incorporation in *L. sakei*. A, *In vivo* detection of intracellular
775 heme molecules through the expression of the *lacZ* gene. The *L. sakei* RV2002 hrtR-lac
776 strain was grown for 1 h in the presence of the indicated concentrations of hemin. β -Gal
777 activity was quantified by luminescence (see “Material and methods”). Mean values are
778 shown (n=7). Error bars represent the standard deviation. B, Quantification of the ^{57}Fe content
779 of the WT (23K) strain grown in the absence and presence of ^{57}Fe -hemin for 1h and 19h. The
780 mean values and range of two independent experiments are shown. RLU, relative light units.